Neuroscience Research 185 (2022) 1–10

Contents lists available at ScienceDirect

Neuroscience Research

journal homepage: www.sciencedirect.com/journal/neuroscience-research

Phldb2 is essential for regulating hippocampal dendritic spine morphology through drebrin in an adult-type isoform-specific manner

Min-Jue Xie [a,b,c,d], Hideshi Yagi [a,e], Tokuichi Iguchi [a,f,g], Hiroyuki Yamazaki [h,i], Kenji Hanamura [h], Hideo Matsuzaki [b,c,d], Tomoaki Shirao [h,j], Makoto Sato [a,b,d,f,*]

[a] Division of Cell Biology and Neuroscience, Department of Morphological and Physiological Sciences, Faculty of Medical Sciences, University of Fukui, Fukui 910-1193, Japan
[b] Division of Development of Mental Functions, Research Center for Child Mental Development, University of Fukui, Fukui 910-1193, Japan
[c] Life Science Innovation Center, University of Fukui, Fukui 910-1193, Japan
[d] United Graduate School of Child Development, Osaka University, Kanazawa University, Hamamatsu University School of Medicine, Chiba University and University of Fukui (UGSCD), Osaka University, Osaka 565-0871, Japan
[e] Department of Cell Biology, Hyogo College of Medicine, Hyogo 663-8501, Japan
[f] Department of Anatomy and Neuroscience, Graduate School of Medicine, Osaka University, Osaka 565-0871, Japan
[g] Department of Nursing, Faculty of Health Science, Fukui Health Science University, Fukui 910-3190, Japan
[h] Department of Neurobiology and Behavior, Gunma University Graduate School of Medicine, Maebashi 371-8511, Japan
[i] Faculty of Social Welfare, Gunma University of Health and Welfare, Maebashi 371-0823, Japan
[j] AlzMed, Inc., Tokyo 113-8485, Japan

ARTICLE INFO

Keywords:
Actin
Drebrin A
LL5β
Phldb2
PIP_3
Spine

ABSTRACT

Morphologically dynamic dendritic spines are the major sites of neuronal plasticity in the brain; however, the molecular mechanisms underlying their morphological dynamics have not been fully elucidated. Phldb2 is a protein that contains two predicted coiled-coil domains and the pleckstrin homology domain, whose binding is highly sensitive to PIP_3. We have previously demonstrated that Phldb2 regulates synaptic plasticity, glutamate receptor trafficking, and PSD-95 turnover. Drebrin is one of the most abundant neuron-specific F-actin-binding proteins that are pivotal for synaptic morphology and plasticity. We observed that Phldb2 bound to drebrin A (adult-type drebrin), but not to drebrin E (embryonic-type drebrin). In the absence of Phldb2, the subcellular localization of drebrin A in the hippocampal spines and its distribution in the hippocampus were altered. Immature spines, such as the filopodium type, increased relatively in the CA1 regions of the hippocampus, whereas mushroom spines, a typical mature type, decreased in *Phldb2*$^{-/-}$ mice. Phldb2 suppressed the formation of an abnormal filopodium structure induced by drebrin A overexpression. Taken together, these findings demonstrate that Phldb2 is pivotal for dendritic spine morphology and possibly for synaptic plasticity in mature animals by regulating drebrin A localization.

1. Introduction

Dendritic spines and synapse stabilization play pivotal roles in higher brain function (Kasai et al., 2010; Ben Zablah et al., 2021). Several neurological disorders accompanied by cognitive deficits, such as autism spectrum disorder, Alzheimer's disease, and Down's syndrome, exhibit abnormal dendritic spine morphology (Mahmood et al., 2018). During the development of the nervous system, the formation of glutamatergic synaptic inputs is characterized by the appearance of thin and/or elongated filopodia-like protrusions of dendritic spines (thin type or filopodia type). Filopodia, which are thin, headless protrusions, are thought to serve as dendritic spine precursors. As development

Abbreviations: AMPA receptor, α-amino-3-hydroxy-5-methyl-4-isoxazolepropionic acid receptor; BDNF, brain-derived neurotrophic factor; TrkB, tropomysin receptor kinase B; CA, Cornus ammonis; GFP, green fluorescent protein; GFP-dr, GFP-drebrin A; IP, immunoprecipitation; LTP, long-term potentiation; MALDI, matrix-assisted laser desorption/ionization; PH, pleckstrin homology; Phldb2, pleckstrin homology-like domain, family B, member 2; PI3K, phosphatidylinositol-3 kinase; PIP_3, phosphatidylinositol 3,4,5-triphosphate; PSD, postsynaptic density protein; TOF/TOF, time-of-flight/time-of-flight.

* Correspondence to: Department of Anatomy and Neuroscience, Osaka University Graduate School of Medicine, Osaka University, Osaka University, Suita, Osaka, Japan.
E-mail address: makosato@anat2.med.osaka-u.ac.jp (M. Sato).

https://doi.org/10.1016/j.neures.2022.09.010
Received 25 March 2022; Received in revised form 16 September 2022; Accepted 21 September 2022
Available online 23 September 2022

proceeds, protrusion motility decreases and subsequently forms mature spines (mushroom type) (Ghani et al., 2017; Helm et al., 2021). However, the mechanisms underlying spine maturation remain unclear. Dendritic spines contain a high concentration of actin (Matus et al., 1982), which plays a central role in spine morphology. In addition, multiple factors, such as drebrin, integrin, and brain-derived neurotrophic factor (BDNF), may play a role in dendritic spine development and remodeling (Koleske, 2013).

Pleckstrin homology-like domain, family B, member 2 (Phldb2), alternatively called LL5β, contains a pleckstrin homology (PH) domain, which binds specifically to phosphatidylinositol 3,4,5-triphosphate (PIP_3). In our previous report, we demonstrated that Phldb2 helps its binding partner, filamin A, translocate to the leading edge of the plasma membrane where PIP_3 accumulates in migrating cells (Takabayashi et al., 2010). The human protein atlas shows that Phldb2 is expressed in almost all tissues, including the brain (https://www.proteinatlas.org/ENSG00000144824-PHLDB2/tissue). In the brain, we recently demonstrated that Phldb2 is expressed in the hippocampus, especially in dendritic spines. Phldb2 regulates synaptic plasticity and the turnover of the glutamate receptor and postsynaptic density protein (PSD)-95 *in vivo* in our newly generated Phldb2 knockout mice (*Phldb2*$^{-/-}$ mice) (Xie et al., 2019). Interestingly, BDNF application facilitates Phldb2 recruitment to the postsynaptic membrane of dendritic spines *via* PIP_3 (Xie et al., 2019). Tropomysin receptor kinase B (TrkB) is the receptor for BDNF, and phosphatidylinositol-3 kinase (PI3K) is activated downstream by the TrkB signaling cascade. BDNF-TrkB signaling has been reported to promote dendritic filopodial motility and synapse formation *via* the activation of PI3K (Luikart et al., 2008) and the BDNF-TrkB axis is essential for structural long-term potentiation (LTP) (Lai et al., 2012; Harward et al., 2016). Furthermore, it has been shown that BDNF contributes to the formation and maturation of spines (Tyler and Pozzo-Miller, 2003; Alonso et al., 2004; Amaral et al., 2007), although the underlying molecular mechanisms of such BDNF function has not been fully elucidated.

Drebrin, an actin-binding protein that forms stable F-actin and is highly accumulated within dendritic spines (Shirao, 1995; Mikati et al., 2013; Koganezawa et al., 2017). Drebrin has two isoforms, embryonic-type drebrin E and adult-type drebrin A, that change during development from E to A (Shirao et al., 1990). Drebrin A plays an important role in spine maturation and synaptic plasticity (Koganezawa et al., 2017).

In the present study, we identified drebrin A as a novel Phldb2-binding protein. Phldb2 was colocalized with drebrin A in the dendritic spine and suppressed the effects of drebrin A overexpression. *Phldb2*$^{-/-}$ mice exhibited changes in dendritic spine morphology and in drebrin A localization.

2. Materials and methods

2.1. Animals

Phldb2 knockout (*Phldb2*$^{-/-}$) C57BL/6J mice (Xie et al., 2019) were housed in an environment with constant temperature and humidity and were provided with food and water *ad libitum*. The day of vaginal plug confirmation was designated embryonic day 0.5 (Iguchi et al., 2021). All the experiments were conducted in compliance with the guidelines for the use of laboratory animals at the University of Fukui, and efforts were made to minimize both the number of animals used and their suffering (Xie et al., 2019).

2.2. Golgi staining

Golgi staining was performed using the FD Rapid Golgistain Kit (PK401, FD NeuroTechnologies, Ellicott City, CA, USA) according to the manufacturer's instructions. Male *Phldb2*$^{+/+}$ and *Phldb2*$^{-/-}$ mice were euthanized on postnatal day 14. Images were acquired using a bright-field Axioplan 2 microscope (Zeiss, Jena, Germany) with a 100 × oil-immersion objective. We collected serial individual optical sections (*z* interval of 0.5 μm). We randomly selected spines from the secondary and tertiary dendrites of Cornus ammonis (CA)1 pyramidal neurons and evaluated their detailed morphology. All dendritic spines were counted for spine types, as previously described (Ghani et al., 2017) using Neurolucida software (MicroBrightField, Williston, USA). The morphology of spines was defined as follows: Spines were classified into 4 categories based on their morphologies as follows: filopodia spine (longer necks and not clear heads), thin spine (small heads and thin long necks), stubby spine (missing/very small neck), and mushroom spine (large bulbous heads and long necks) (Ghani et al., 2017). While adjusting the focus, we defined the morphology and type of each spine. For the quantification of the spine density, the number of spines was measured per 1 μm dendrite length in the neurons. Data were obtained from three *Phldb2*$^{+/+}$ and *Phldb2*$^{-/-}$ mice each. Five neurons were randomly selected from each mouse and five apical or basal dendrites were chosen from each neuron subsequently. The number of spines counted was as follows: 2449 spines (apical dendrites of the *Phldb2*$^{+/+}$ mice), 2213 spines (apical dendrites of the *Phldb2*$^{-/-}$ mice), 2821 spines (basal dendrites of *Phldb2*$^{+/+}$ mice), and 2516 spines (basal dendrites of *Phldb2*$^{-/-}$ mice).

2.3. Cell culture and DNA transfection

Primary hippocampal neurons were prepared at embryonic day 17.5 as previously described (Xie et al., 2019). COS-7 cells were maintained in Dulbecco's modified Eagle's medium (Invitrogen, Grand Island, NY) containing 10% fetal bovine serum at 37 °C in 5 % CO_2. Notably, 2 μg of expression vectors per 6 cm dish were transfected with FuGENE 6 transfection reagent (Roche Diagnostics Corporation, Indianapolis, IN, USA). One μg Green fluorescent protein (GFP)-drebrin A, GFP-drebrin E, various GFP-tagged fragments of drebrin (GFP-drs) (Hayashi and Shirao, 1999), and 1 μg myc-Phldb2 expression vectors (Xie et al., 2019) were co-transfected into COS-7 cells. The cells were lysed at 48 h after transfection. 0.1 μg GFP, GFP-drebrin A, GFP-drebrin E and 0.3 μg myc-Phldb2 expression vectors (Xie et al., 2019) and 0.2 μg tdTomato were co-transfected into primary hippocampal neurons.

2.4. Immunoprecipitation (IP) and western blot

Cell culture or hippocampi were lysed in RIPA buffer (0.1 % sodium deoxycholate, 0.5 % Nonidet P-40, 150 mM NaCl, 50 mM Tris-HCl with 1 % protease inhibitor cocktail). Insoluble materials were removed from the lysate by ultracentrifugation (60 min centrifugation at 100,000 × *g*) prior to the IP experiments. Co-IP was performed using antibody-bound Dynabeads protein G (Invitrogen). The samples were incubated with antibodies for 2 h at 4 °C. Subsequently, the dynabeads were washed three times in ice-cold RIPA buffer and boiled in SDS sample buffer. The resulting samples were resolved using SDS-PAGE. The proteins were subjected to western blot analysis. The following antibodies were used: anti-myc (1:200, sc-40, Santa Cruz Biotechnology, CA), anti-GFP (1:1000, 598, MBL, Nagoya, Japan), anti-drebrin (it recognizes both drebrin A and drebrin E) (1:100, Shirao and Obata, 1986), β-actin (1:2000, PM053-7, MBL), GAPDH (1:4000, M171-7, MBL) and mouse anti-Phldb2 (1:100, Xie et al., 2019). To search for the Phldb2-binding protein, we performed IP using the cerebral cortex at embryonic day 17.5 with an anti-Phldb2 antibody. Subsequently, immunoprecipitated samples were subjected to SDS-PAGE gel separation. The gels were stained with Coomassie brilliant blue, and the stained bands were dissected out from the gel and analyzed using matrix-assisted laser desorption/ionization (MALDI) time-of-flight/time-of-flight (TOF/TOF) high-resolution tandem mass spectrometry (Bruker Daltonics, Bremen, Germany) (Kubo et al., 2010). For peptide mass fingerprinting identification, the tryptic mass maps were transferred with MS Bio Tools (Bruker Daltonics) as input to search the National Center for

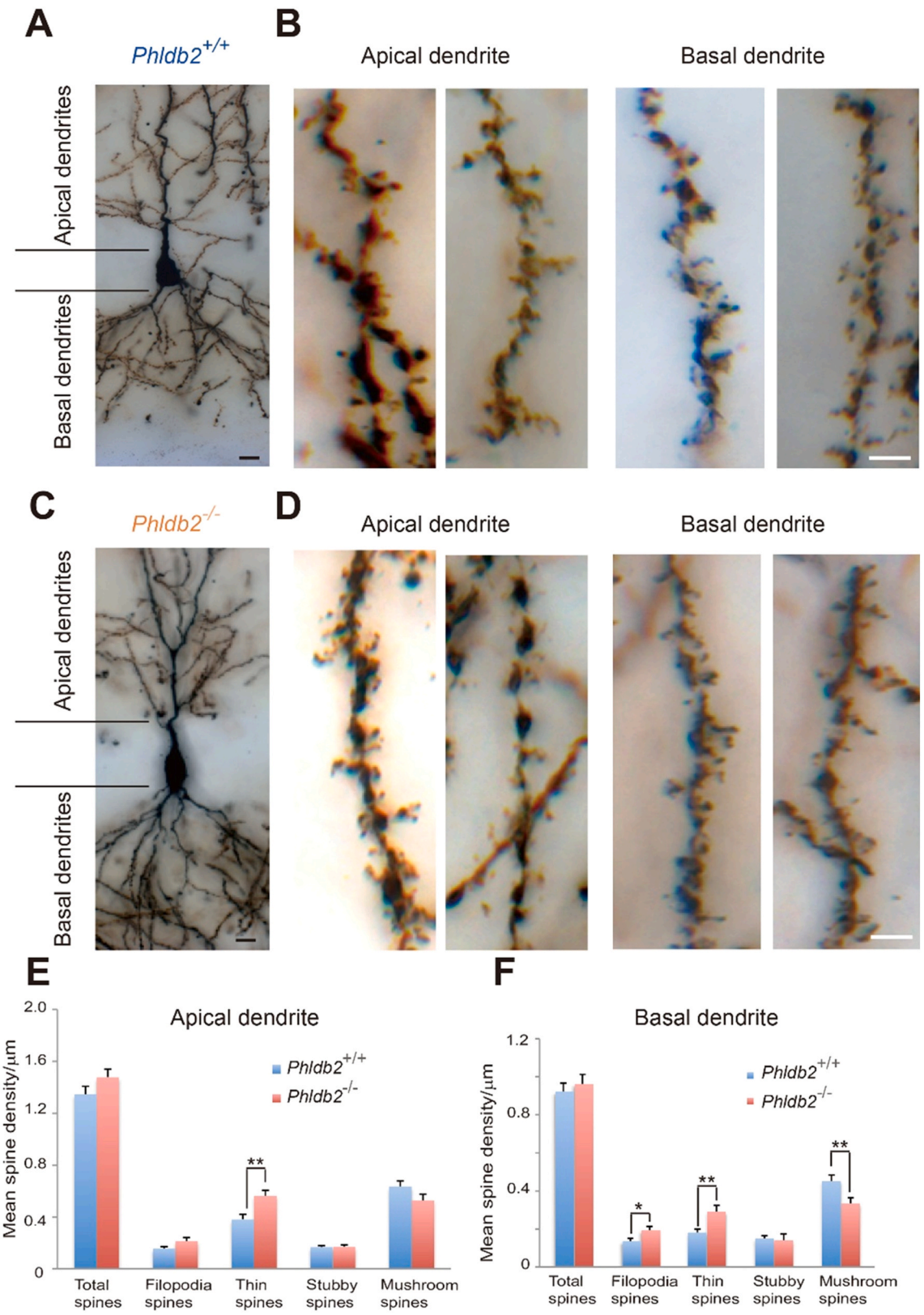

Fig. 1. Deletion of Phldb2 expression results in changes in dendritic spine morphology. Golgi staining was performed in hippocampal CA1 pyramidal neurons of *Phldb2*$^{+/+}$ (A, B) and *Phldb2*$^{-/-}$ mice (C, D) at postnatal day 14. Higher magnification images of apical and basal dendrites are shown in (B) and (D). Scale bars = 10 μm (A, C) and 5 μm (B, D). (E, F) Quantification of spine density (number of spines per 1 μm of dendrite length). Deletion of Phldb2 resulted in an increase in the number of filopodia and thin spines, and a decrease in the number of mushroom spines in basal dendrites (n = 3 mice for each genotype. Five dendrites/mice were analyzed. Apical dendrites: *Phldb2*$^{+/+}$ mice, n = 2449 spines; *Phldb2*$^{-/-}$ mice, n = 2213 spines. Basal dendrites: *Phldb2*$^{+/+}$ mice, n = 2821 spines; *Phldb2*$^{-/-}$ mice, n = 2516 spines. Mean ± SEM. Student's *t*-test, $^{*}P < 0.05$, $^{**}P < 0.01$).

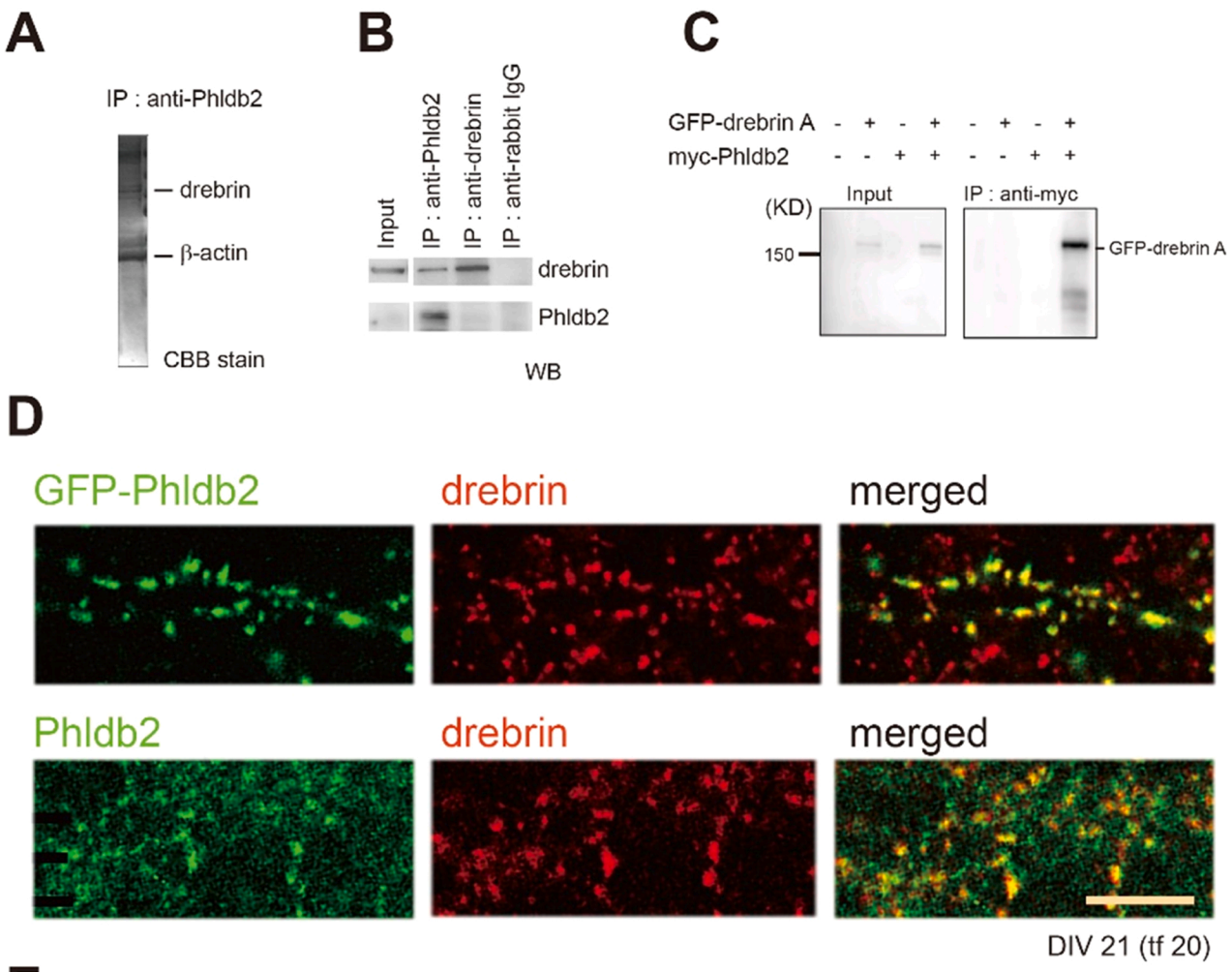

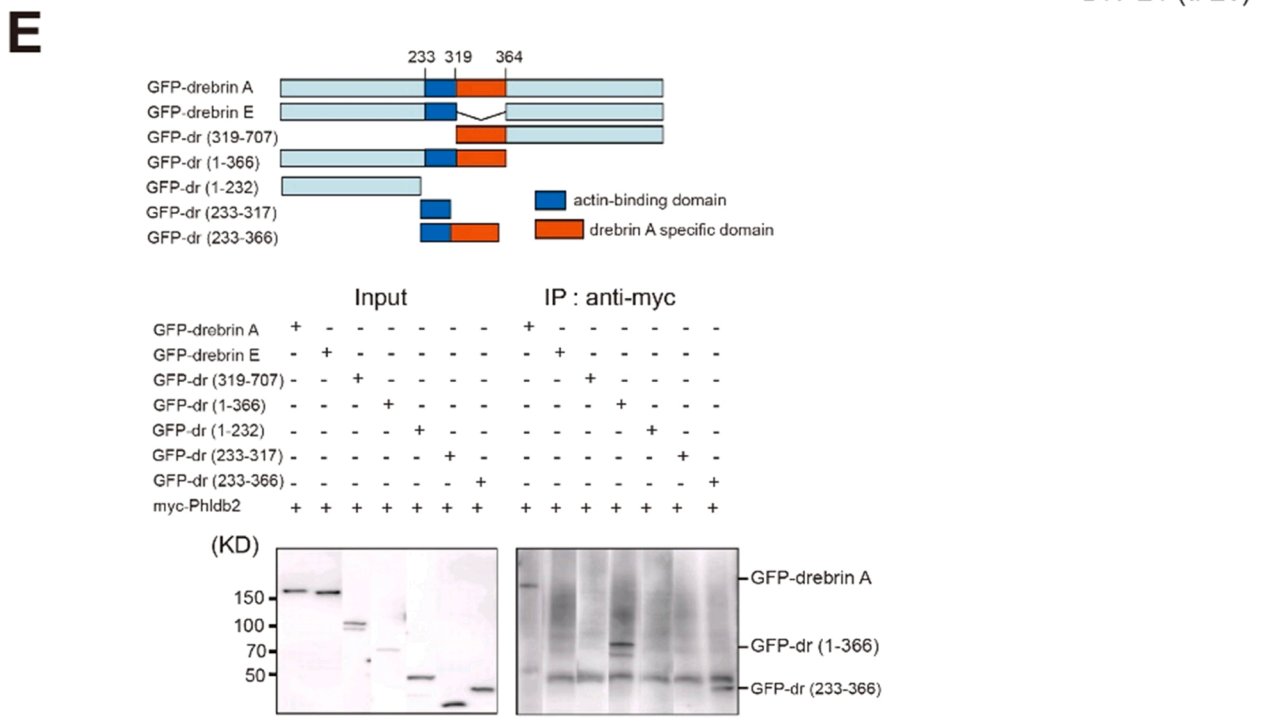

(caption on next page)

Fig. 2. Phldb2 interacts with drebrin A, but not drebrin E *via* the drebrin A-specific domain. (A) Immunoprecipitation (IP) using the *Phldb2*$^{+/+}$ mouse brain with anti-Phldb2 antibody. Immunoprecipitates were separated, subjected to SDS-PAGE, and gels were stained with Coomassie Brilliant Blue (CBB). Stained bands were dissected from the gel and analyzed using matrix-assisted laser desorption/ionization (MALDI) time-of-flight/time-of-flight (TOF/TOF) high-resolution tandem mass spectrometry, and drebrin was identified. (B) IP was performed using hippocampal tissues of postnatal day 14 mouse with anti-Phldb2 and anti-drebrin antibodies. Anti-IgG antibody was used as a negative control. (C) GFP-drebrin A and myc-Phldb2 expression vectors were co-transfected into COS-7 cells. Lysates were subjected to immunoprecipitation with an anti-myc antibody and visualized using an anti-GFP antibody. GFP-drebrin A was co-immunoprecipitated with Phldb2. (D) Cultured hippocampal neurons were transfected (tf) with or without GFP-Phldb2 expression vector at day 20 *in vitro* (DIV 20) and fixed at DIV 21. Exogenous GFP-Phldb2 (upper row) and endogenous Phldb2 (lower row) were accumulated in spines. Yellow areas are overlapped areas of drebrin (red fluorescence) and Phldb2 (green fluorescence), indicating these molecules are co-localized there. Scale bars = 10 μm. (E) Schematic drawings showing the full-length and truncated mutants of GFP-drebrin (GFP-dr). To determine the region of Phldb2 responsible for drebrin A binding, myc-Phldb2 and GFP-drs were co-expressed in COS-7 cells. The lysates were then subjected to immunoprecipitation with an anti-myc antibody. GFP-drebrin A, GFP-dr (1–366), and GFP-dr (233–366) were detected in immunoprecipitates.

Biotechnology Information (NCBI) database with the Mascot software (Matrix Science, Boston, MA).

2.5. Immunostaining

Primary neuronal cultures were fixed with 4 % paraformaldehyde and staining was performed as previously described (Xie et al., 2013). For immunohistochemistry, the mice were perfused for 1 min with phosphate-buffered saline, followed by 12 min of perfusion with 0.1 M phosphate buffer containing 4 % paraformaldehyde at a rate of 5 mL/min. The perfused brains were placed in ice-cold 30 % sucrose solution in PBS and maintained at 4 °C overnight. Sections of 20 μm were cut and incubated overnight at 4 °C with a primary antibody. Images were obtained using an LSM 5 PASCAL confocal microscope (Carl Zeiss MicroImaging GmbH, Jena, Germany) or an all-in-one fluorescence microscope BZ-X800 (Keyence Corporation, Osaka, Japan) and were analyzed with ImageJ software (Rasband, W.S., ImageJ, U.S. National Institutes of Health, Bethesda, MA, http://imagej.nih.gov/ij/, 1997–2015) to measure a plot of the fluorescence intensity profile. The following antibodies were used: anti-myc (1:100, sc-40, Santa Cruz Biotechnology, CA), anti-drebrin (1:10, Shirao and Obata, 1986), rabbit anti-drebrin A (1:50, Aoki et al., 2005), and mouse anti-Phldb2 (1:50, Xie et al., 2019).

2.6. Statistics

All the statistical analyses were performed using the IBM SPSS Statistics 23 and JMP Pro 14. Pairwise comparisons between groups were conducted using a two-tailed Student's *t*-test, one-way analysis of variance (ANOVA) and Tukey's post-hoc tests and two-way repeated measures ANOVA. The null hypothesis was rejected at $P < 0.05$. Quantitative data are presented as mean ± SEM.

3. Results

3.1. Deletion of Phldb2 resulted in the dominance of immature spines in the hippocampus

Phldb2 is a binding partner of the well-known actin-cross-linking protein, filamin A (Takabayashi et al., 2010) and actin is essential for the formation and morphological regulation of the dendritic spines (Fischer et al., 1998). In addition, BDNF application facilitates Phldb2 recruitment to the postsynaptic membrane of the dendritic spines (Xie et al., 2019). We first investigated whether Phldb2 affects the dendritic spine morphology.

We examined the spine morphology in the CA1 regions of the hippocampus of *Phldb2*$^{-/-}$ mice using Golgi staining (Supplementary Fig. 1 and Fig. 1A–D). For apical dendrites, the proportion of thin spines was significantly increased in *Phldb2*$^{-/-}$ mice. The mean density of the total spines (number of spines per 1 μm of dendrite length) was as follows: *Phldb2*$^{+/+}$ mice, 1.35 ± 0.06; *Phldb2*$^{-/-}$ mice, 1.48 ± 0.06, *P* value between these two results was 0.148 ($P = 0.148$); that of filopodia spines: *Phldb2*$^{+/+}$ mice, 0.16 ± 0.01; *Phldb2*$^{-/-}$ mice, 0.21 ± 0.03, $P = 0.06$; that of thin spines: *Phldb2*$^{+/+}$ mice, 0.38 ± 0.04; *Phldb2*$^{-/-}$ mice, 0.56 ± 0.04, $P = 0.004$; that of stubby spines: *Phldb2*$^{+/+}$ mice, 0.17 ± 0.01, *Phldb2*$^{-/-}$ mice, 0.17 ± 0.01, $P = 0.889$; and that of mushroom spines: *Phldb2*$^{+/+}$ mice, 0.64 ± 0.04, *Phldb2*$^{-/-}$ mice, 0.53 ± 0.05, $P = 0.101$.) (Fig. 1E). In the basal dendrites, we found that the proportion of immature spines (filopodia and thin spines) increased, while the proportion of mature spines (mushroom spine) decreased (the mean density of the total spines: *Phldb2*$^{+/+}$ mice, 0.92 ± 0.04, *Phldb2*$^{-/-}$ mice, 0.96 ± 0.05, $P = 0.540$; that of filopodia spines: *Phldb2*$^{+/+}$ mice, 0.14 ± 0.02; *Phldb2*$^{-/-}$ mice, 0.19 ± 0.02, $P = 0.019$; that of thin spines: *Phldb2*$^{+/+}$ mice, 0.18 ± 0.02, *Phldb2*$^{-/-}$ mice, 0.29 ± 0.03, $P = 0.002$; that of stubby spines: *Phldb2*$^{+/+}$ mice, 0.15 ± 0.01, *Phldb2*$^{-/-}$ mice, 0.14 ± 0.03, $P = 0.654$; and that of mushroom spines: *Phldb2*$^{+/+}$ mice, 0.45 ± 0.03, *Phldb2*$^{-/-}$ mice, 0.33 ± 0.03, $P = 0.006$.) (Fig. 1F). These results suggest that Phldb2 plays an important role in dendritic spine maturation.

3.2. Phldb2 binds to drebrin A, but not drebrin E, and regulates the subcellular localization of drebrin A in the spine

Since Phldb2 is potentially involved in cytoskeletal regulation, we searched for its binding partners, in addition to filamin A (Takabayashi et al., 2010) to elucidate how Phldb2 regulates the morphology of the dendritic spines, because expression of filamin A is very poor in mature spines (Noam et al., 2012; Yagi et al., 2014). We performed IP using mouse brains with an anti-Phldb2 antibody. The resultant Phldb2-binding proteins were analyzed using mass spectrometry. Drebrin was identified as one of the Phldb2-binding proteins (Fig. 2A). In addition, we also identified actinin α4 and vimentin as binding proteins. We first isolated β-actin, however, we could not confirm its direct binding with Phldb2 in the COS-7 cells, suggesting that their direct binding is unlikely (Supplementary Fig. 2). We will focus on drebrin in this study. We confirmed by co-IP assays the presence of the Phldb2/drebrin complex in hippocampal tissues of postnatal day 14 mice (Fig. 2B) and as well as in COS-7 cells in which the GFP-drebrin A and myc-Phldb2 expression vectors were co-transfected (Fig. 2C). Immunocytochemically, co-localization of drebrin and Phldb2 was observed in the spines of the hippocampal neurons (Fig. 2D).

Drebrin is a major actin-binding protein in the brain that is involved in spine maturation (Takahashi et al., 2003). There are two major drebrin isoforms, an embryonic-type isoform (drebrin E) and an adult-type isoform (drebrin A) (Shirao, 1995; Koganezawa et al., 2017). We observed that Phldb2 bound to drebrin A, but not to drebrin E (Fig. 2E). To identify the regions of drebrin A responsible for the interaction with Phldb2, we used a series of deletion mutants of drebrin A. The actin binding and drebrin A-specific domains [GFP-drebrin A, GFP-dr (1–366) and GFP-dr (233–366)] were crucial for the interaction of drebrin A with Phldb2 (Fig. 2E). It has been shown that the overexpression of drebrin A or drebrin E results in the elongation of dendritic spines (Biou et al., 2008; Hayashi and Shirao, 1999); subsequently, we examined whether Phldb2 regulates the function of drebrin A. While the overexpression of drebrin A induced the elongation of dendritic spines in the cultured hippocampal neurons, remarkably in *Phldb2*$^{-/-}$ mice (Fig. 3A, B and Supplementary Fig. 3, middle row and Fig. 3C), overexpression of

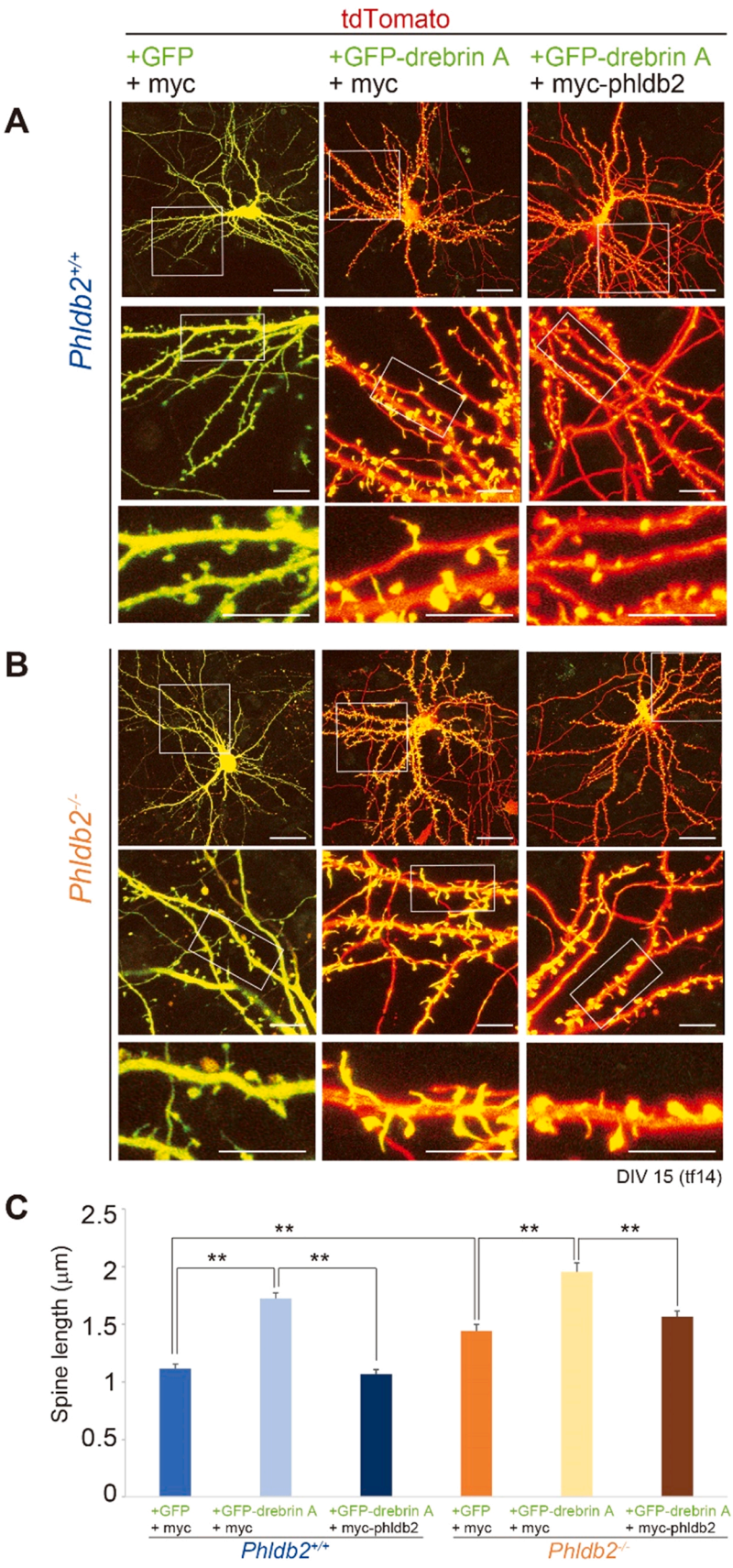

Fig. 3. Phldb2 suppresses the elongation of dendritic spines induced by drebrin A overexpression. Cultured hippocampal neurons were transfected with GFP, GFP-drebrin A, tdTomato and myc-phldb2 expression vectors at day 14 *in vitro* and fixed at DIV15. *Phldb2*$^{+/+}$ (A) and *Phldb2*$^{-/-}$ mice (B). Scale bars = 40 μm (upper row) and 10 μm (middle and lower rows). Sole tdTomato channel images (red) are shown as Supplementary Fig. 3. (C) Distance from the bottom of the spine neck to the uppermost border of the spine head was measured and shown as the spine length. Quantification of spine length (n = 3 neurons for each type. *Phldb2*$^{+/+}$ mice: GFP + myc, n = 163 spines; GFP-drebrin A + myc, n = 141 spines; GFP-drebrin A + myc-phldb2, n = 175 spines. *Phldb2*$^{-/-}$ mice: GFP + myc, n = 152 spines; GFP-drebrin A + myc, n = 134 spines; GFP-drebrin A + myc-phldb2, n = 131 spines. Mean ± SEM. One-way ANOVA with post-hoc Tukey HSD, $^{**}P < 0.001$).

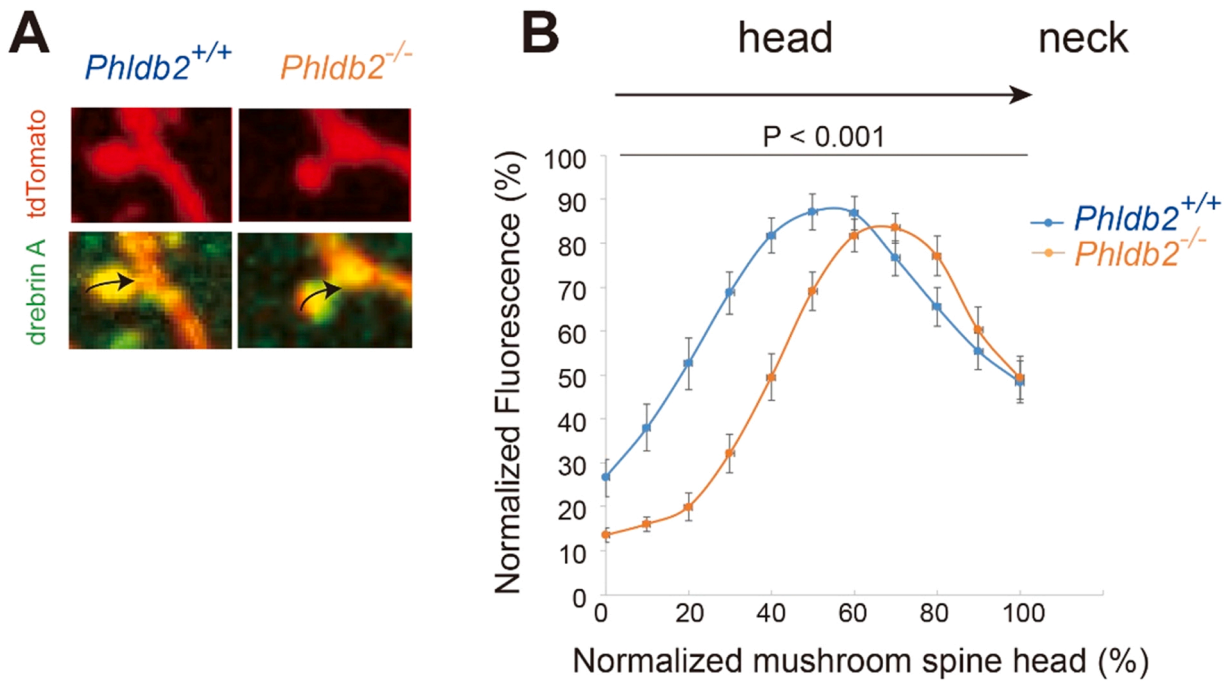

Fig. 4. Phldb2 regulates drebrin A localization in the spine. (A) Hippocampal neurons were transfected with tdTomato expression vectors and fixed on day 21 *in vitro* (DIV 21). Endogenous drebrin A was stained (green). (B) The fluorescence intensity profiles along black arrows were plotted. The spine head along the black arrow was divided into 10 bins and normalized fluorescence intensities at each bin are shown. For normalization, the signal intensity of the dendritic spine head bin was divided by the peak intensity (intensity/peak intensity ratio). Relative locations of each bin in the spine head are shown on the X-axis (0–100 %). The fluorescence peak of drebrin A in the spine head in *Phldb2*$^{-/-}$ mice was closer to the neck than that in *Phldb2*$^{+/+}$ mice (*Phldb2*$^{+/+}$ mice, n = 26 spines; *Phldb2*$^{-/-}$ mice, n = 27 spines). Mean ± SEM. Two-way repeated-measures ANOVA, $F_{(1,51)} = 0.548$, $P < 0.001$).

Phldb2 rescued the effects induced by drebrin A (Fig. 3A, B, and Supplementary Fig. 3, right row and Fig. 3C and Supplementary Fig. 4A). In the following measurements, we measured the distance from the bottom of the spine neck to the uppermost border of the spine head and presented as the spine length. The mean spine length in *Phldb2*$^{+/+}$ mice: GFP-drebrin A + myc, 1.72 ± 0.05 μm; GFP-drebrin A + myc-phldb2, 1.34 ± 0.03 μm. The mean spine length in *Phldb2* $^{-/-}$ mice: GFP-drebrin A + myc, 1.96 ± 0.08 μm; GFP-drebrin A + myc-phldb2, 1.60 ± 0.05 μm (Fig. 3A, B). However, overexpression of Phldb2 did not rescue the long dendritic spines induced by drebrin E overexpression of drebrin E (Supplementary Fig. 4B). In addition, the mean spine length in *Phldb2*$^{-/-}$ mice was longer than that in *Phldb2*$^{+/+}$ mice, which is consistent with the Golgi staining results (Fig. 1, Fig. 3A, B, left row, and Fig. 3C). The mean spine length in *Phldb2*$^{+/+}$ mice was 0.11 ± 0.04 μm, whereas that in *Phldb2*$^{-/-}$ mice was 1.45 ± 0.05 μm.

3.3. *Phldb2 regulates the localization and expression of drebrin A*

We previously demonstrated that Phldb2 regulates the localization of PSD-95, a pivotal postsynaptic scaffolding protein in excitatory neurons (Xie et al., 2019). Drebrin governs spine morphogenesis and synaptic PSD-95 clustering (Takahashi et al., 2003). Since Phldb2 interacts with drebrin A, we subsequently queried whether Phldb2 regulates the localization of drebrin A in the spines. The distribution of drebrin A throughout the spine was measured and analyzed. Drebrin A location was eccentrically shifted towards the dendritic shaft in *Phldb2*$^{-/-}$ mice compared to that in *Phldb2*$^{+/+}$ mice (Fig. 4), suggesting that Phldb2 helped drebrin A localize to the spine head.

Subsequently, we investigated whether Phldb2 regulates drebrin A expression in the hippocampus *in vivo*. Immunohistochemical analysis showed that the fluorescence intensity of drebrin A was higher in the hippocampi of *Phldb2*$^{-/-}$ mice (Fig. 5A–C). In the stratum oriens, drebrin A expression was stronger in *Phldb2*$^{-/-}$ mice than in *Phldb2*$^{+/+}$ mice (*Phldb2*$^{+/+}$ mice, 1.02 ± 0.04; *Phldb2*$^{-/-}$ mice, 1.27 ± 0.04, $P < 0.001$) (Fig. 5C). In addition, western blotting analysis demonstrated that drebrin A expression was higher in *Phldb2*$^{-/-}$ than in *Phldb2*$^{+/+}$ mice (Fig. 5D, E).

4. Discussion

The F-actin side-binding protein drebrin is involved in the formation and maintenance of dendritic spines in the brain and plays a role in higher brain functions such as memory formation (Koganezawa et al., 2017; Shirao et al., 2017). Drebrin A is the major isoform of drebrin in the adult brain and is highly concentrated in dendritic spines, where it regulates spine morphology and synaptic plasticity. Conversely, drebrin E is the major isoform in the embryonic brain that regulates neuronal morphological differentiation and chain migration of neuroblasts (Kajita et al., 2017; Shirao et al., 2017). The binding of Phldb2 to drebrin A (adult type), but not drebrin E (embryonic type), indicates that the influence of Phldb2 on actin filaments changes as development progresses.

It is generally accepted that the immature type of spines are filopodia, thin or stubby spines, whereas the mature type of spines are mushroom spines (Berry and Nedivi, 2017; Helm et al., 2021). The overexpression of drebrin A induces spine elongation in immature and mature neurons (Hayashi and Shirao, 1999; Mizui et al., 2005) and this abnormal phenotype was rescued by exogenous Phldb2. Deletion of Phldb2 resulted in an increase in immature spines, especially in basal dendrite areas (*i.e.*, stratum oriens in the hippocampus). Given the amount of drebrin A increases in the basal dendrite areas of *Phldb2*$^{-/-}$ mice, we could not exclude the possibility of Phldb2 being involved in drebrin A degradation and/or translocation out of the spines.

We observed that Phldb2 controls the distribution of drebrin A in the spine, suggesting that drebrin A accumulation at postsynaptic sites depends on Phldb2. Thus, it is likely that the adult-type isoform-specific function of drebrin in neurotransmission (Kojima et al., 2016) is regulated by Phldb2. Long-term potentiation (LTP) stimulation induces rapid drebrin A-actin exodus in dendritic spines (Mizui et al., 2014) and LTP is

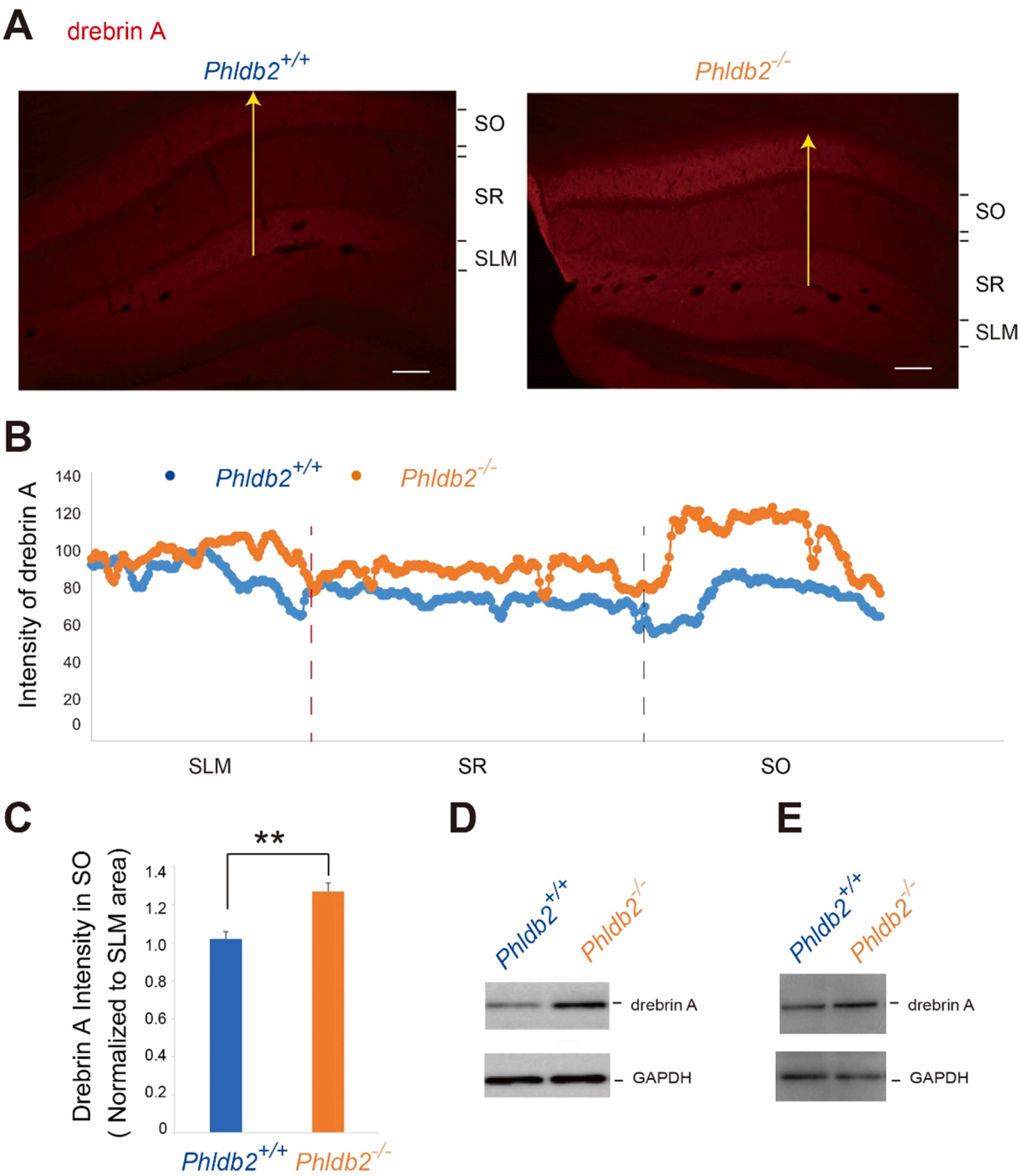

Fig. 5. Phldb2 deletion results in an increase in the drebrin A expression in the hippocampus. (A) The expression of drebrin A was detected in the hippocampus using immunohistochemistry. Scale bar = 100 μm. (B) Example plots of the fluorescence intensity profiles of drebrin A along the yellow line from the stratum lacunosum-moleculare (SLM) to the stratum oriens (SO). Drebrin A was more abundant in the SO of *Phldb2*$^{-/-}$ mice than in that of *Phldb2*$^{+/+}$ mice. (C) The fluorescence intensity of drebrin A expression in SO was semi-quantified using Image J. Relative fluorescence intensity, namely, fluorescence intensity in SO against SLM, was measured in each case and summarized. (n = 3 mice for each genotype. Twelve slices were analyzed. Mean ± SEM. Student's *t*-test, $^{**}P < 0.01$). (D) The expression of drebrin A was analyzed by western blotting using cultured hippocampal neurons at day 18 *in vitro* (DIV 18). (E) Western blotting analyses with hippocampal tissues from 4 months mice. GAPDH was used as an internal control.

impaired in adult drebrin A-knockout mice (Kojima et al., 2016). We previously demonstrated that Phldb2 regulates AMPA receptor localization in the synaptic membrane, and Phldb2 deficiency results in LTP impairment (Xie et al., 2019). The Phldb2-drebrin-F actin network is likely to play an important role in the structure and function of the synapses.

Since drebrin A localization changed between the absence or presence of Phldb2, we assumed that Phldb2 is capable of controlling the localization of drebrin A: Phldb2 binds to PIP_3, which works just by the synaptic membrane, and regulates the localization of drebrin A, AMPA receptor, and PSD-95 in dendritic spines (Xie et al., 2019). In contrast, drebrin binds to F-actin, which is mainly localized in the dendritic shaft and spine neck (Shirao, 1995; Van Bommel et al., 2019). This indicates that Phldb2 is upstream of drebrin A. However, it is apparent that

Phldb2 and drebrin interact and form a molecular complex. Therefore, we cannot exclude the possibility that drebrin A also regulates Phldb2 localization. Thus, drebrin A may function as an upstream molecule for Phldb2. We believe that the concept of upstream and/or downstream comes from the concept of a signaling cascade, where the upstream molecule governs the downstream molecules. However, as mentioned above, since these two molecules may form a complex, we cannot conclude that one is the absolute upstream and the other downstream; rather, they mutually control each other.

Several lines of evidence indicate that drebrin interacts with many molecules, such as PSD-95, homers, and PTEN, in addition to actin, owing to its versatile functions in the spine: (1) Drebrin regulates PSD-95 (Koganezawa et al., 2017), whereas Phldb2 binds to PSD-95 and regulates its localization and turnover (Xie et al., 2019). (2) Homer is an important and highly abundant scaffold protein in dendritic spines. Previous reports have shown a potential regulatory role of Homer in modulating excitatory synaptic spine homeostatic scaling *via* binding to drebrin, and the Homer tetramer promotes the actin-bundling activity of drebrin (Li et al., 2019). (3) Phldb2 binds to PIP_3 with a very high sensitivity and responds to BDNF (Xie et al., 2019). It should be noted that PIP_3 is generated in the downstream signaling cascades of BNDF receptor, TrkB (Luikart et al., 2008). The phosphatase and tensin homolog (PTEN), which dephosphorylates PIP_3 to PIP_2, binds to drebrin (Kreis et al., 2013). Neuronal activity induces dissociation of the PTEN/drebrin complex (Kreis et al., 2013). The significance of Phldb2-drebrin should be explored in all these events.

We identified actinin α4 as a Phldb2-binding candidate. Actinin works, in a sense, as a linker between NMDA receptor and actin fibers (Nakagawa et al., 2004). How Phldb2 exerts its activities with drebrin and/or actinin in the spine is also a subject of future investigation.

5. Conclusion

Phldb2 is essential for regulating hippocampal dendritic spine morphology by controlling the localization and expression of drebrin in an adult-type isoform (drebrin A)-specific manner.

CRediT authorship contribution statement

Min-Jue Xie: performed almost all the experiments. **Hideshi Yagi:** generated knockout mice. **Tokuichi Iguchi:** generated knockout mice and advised on the experimental conditions for the primary culture of neurons. **Hiroyuki Yamazaki, Kenji Hanamura, and Tomoaki Shirao:** provided the drebrin vector and drebrin antibody, and advised on the experimental conditions for drebrin. **Hideo Matsuzaki:** advised about some experimental conditions. **Makoto Sato:** conceived the project, directed the research, and wrote the manuscript along with **Min-Jue Xie**. All listed members provided invaluable comments on the article and contributed to the final version of the manuscript.

Statement of ethics

The authors have no ethical conflicts to disclose.

Declaration of Competing Interest

The authors declare that they have no known competing financial interests or personal relationships that could influence the work reported in this study.

Data Availability

No data was used for the research described in the article.

Acknowledgements

We are grateful to S. Kanae, I. Kumano, Y. Sasaki, and H. Miyagoshi for technical assistance and to T. Taniguchi for secretarial assistance and Y. Fukazawa for critical reading on the manuscript. This work was supported in part by the Uehara Memorial Foundation, Takeda Science Foundation, Takeda Medical Research Foundation, Novartis Stiftung für Medizinisch-Biologische Forschung (Novartis Foundation for Medical-Biological Research), and Kakenhi, from the Ministry of Education, Culture, Sports, Science and Technology (MEXT) of Japan (25293043 and 17H04014 to Makoto Sato, 15k08151 and 23590232 to Min-Jue Xie).

Appendix A. Supporting information

Supplementary data associated with this article can be found in the online version at doi:10.1016/j.neures.2022.09.010.

References

Alonso, M., Medina, J.H., Pozzo-Miller, L., 2004. ERK1/2 activation is necessary for BDNF to increase dendritic spine density in hippocampal CA1 pyramidal neurons. Learn. Mem. 11, 172–178.
Amaral, M.D., Chapleau, C.A., Pozzo-Miller, L., 2007. Transient receptor potential channels as novel effectors of brain-derived neurotrophic factor signaling: potential implications for Rett syndrome. Pharm. Ther. 113, 394–409.
Aoki, C., Sekino, Y., Hanamura, K., Fujisawa, S., Mahadomrongkul, V., Ren, Y., Shirao, T., 2005. Drebrin A is a postsynaptic protein that localizes in vivo to the submembranous surface of dendritic sites forming excitatory synapses. J. Comp. Neurol. 483, 383–402.
Ben Zablah, Y., Zhang, H., Gugustea, R., Jia, Z., 2021. LIM-kinases in synaptic plasticity, memory, and brain diseases. Cells 10, 2079.
Berry, K.P., Nedivi, E., 2017. Spine dynamics: are they all the same? Neuron 96, 43–55.
Biou, V., Brinkhaus, H., Malenka, R.C., Matus, A., 2008. Interactions between drebrin and Ras regulate dendritic spine plasticity. Eur. J. Neurosci. 27, 2847–2859.
Fischer, M., Kaech, S., Knutti, D., Matus, A., 1998. Rapid actin-based plasticity in dendritic spines. Neuron 20, 847–854.
Ghani, M.U., Mesadi, F., Kanık, S.D., Argunşah, A.Ö., Hobbiss, A.F., Israely, I., Ünay, D., Taşdizen, T., Çetin, M., 2017. Dendritic spine classification using shape and appearance features based on two-photon microscopy. J. Neurosci. Methods 279, 13–21.
Harward, S.C., Hedrick, N.G., Hall, C.E., Parra-Bueno, P., Milner, T.A., Pan, E.H., Laviv, T., Hempstead, B.L., Yasuda, R., McNamara, J.O., 2016. Autocrine BDNF-TrkB signaling within a single dendritic spine. Nature 538, 99–103.
Hayashi, K., Shirao, T., 1999. Change in the shape of dendritic spines caused by overexpression of drebrin in cultured cortical neurons. J. Neurosci. 19, 3918–3925.
Helm, M.S., Dankovich, T.M., Mandad, S., Rammner, B., Jähne, S., Salimi, V., Koerbs, C., Leibrandt, R., Urlaub, H., Schikorski, T., Rizzoli, S.O., 2021. A large-scale nanoscopy and biochemistry analysis of postsynaptic dendritic spines. Nat. Neurosci. 24, 1151–1162.
Iguchi, T., Oka, Y., Yasumura, M., Omi, M., Kuroda, K., Yagi, H., Xie, M.J., Taniguchi, M., Bastmeyer, M., Sato, M., 2021. Mutually repulsive EphA7-EfnA5 organize region-to-region corticopontine projection by inhibiting collateral extension. J. Neurosci. 41, 4795–4808.
Kajita, Y., Kojima, N., Koganezawa, N., Yamazaki, H., Sakimura, K., Shirao, T., 2017. Drebrin E regulates neuroblast proliferation and chain migration in the adult brain. Eur. J. Neurosci. 46, 2214–2228.
Kasai, H., Hayama, T., Ishikawa, M., Watanabe, S., Yagishita, S., Noguchi, J., 2010. Learning rules and persistence of dendritic spines. Eur. J. Neurosci. 32, 241–249.
Koganezawa, N., Hanamura, K., Sekino, Y., Shirao, T., 2017. The role of drebrin in dendritic spines. Mol. Cell. Neurosci. 84, 85–92.
Kojima, N., Yasuda, H., Hanamura, K., Ishizuka, Y., Sekino, Y., Shirao, T., 2016. Drebrin A regulates hippocampal LTP and hippocampus-dependent fear learning in adult mice. Neuroscience 324, 218–226.
Koleske, A.J., 2013. Molecular mechanisms of dendrite stability. Nat. Rev. Neurosci. 14, 536–550.
Kreis, P., Hendricusdottir, R., Kay, L., Papageorgiou, I.E., van Diepen, M., Mack, T., Ryves, J., Harwood, A., Leslie, N.R., Kann, O., Parsons, M., Eickholt, B.J., 2013. Phosphorylation of the actin binding protein Drebrin at S647 is regulated by neuronal activity and PTEN. PLoS One 8, e71957.
Kubo, E., Hasanova, N., Tanaka, Y., Fatma, N., Takamura, Y., Singh, D., Akagi, Y., 2010. Protein expression profiling of lens epithelial cells from Prdx6-depleted mice and their vulnerability to UV radiation exposure. Am. J. Physiol. Cell Physiol. 298, C342–C354.
Lai, K.O., Wong, A.S., Cheung, M.C., Xu, P., Liang, Z., Lok, K.C., Xie, H., Palko, M.E., Yung, W.H., Tessarollo, L., Cheung, Z.H., Ip, N.Y., 2012. TrkB phosphorylation by Cdk5 is required for activity-dependent structural plasticity and spatial memory. Nat. Neurosci. 15, 1506–1515.

Li, Z., Liu, H., Li, J., Yang, Q., Feng, Z., Li, Y., Yang, H., Yu, C., Wan, J., Liu, W., Zhang, M., 2019. Homer tetramer promotes actin bundling activity of drebrin. Structure 27, 27–38.
Luikart, B.W., Zhang, W., Wayman, G.A., Kwon, C.H., Westbrook, G.L., Parada, L.F., 2008. Neurotrophin-dependent dendritic filopodial motility: a convergence on PI3K signaling. J. Neurosci. 28, 7006–7012.
Mahmood, U., Ahn, S., Yang, E.J., Choi, M., Kim, H., Regan, P., Cho, K., Kim, H.S., 2018. Dendritic spine anomalies and PTEN alterations in a mouse model of VPA-induced autism spectrum disorder. Pharm. Res. 128, 110–121.
Matus, A., Ackermann, M., Pehling, G., Byers, H.R., Fujiwara, K., 1982. High actin concentrations in brain dendritic spines and postsynaptic densities. Proc. Natl. Acad. Sci. USA 79, 7590–7594.
Mikati, M.A., Grintsevich, E.E., Reisler, E., 2013. Drebrin-induced stabilization of actin filaments. J. Biol. Chem. 288, 19926–19938.
Mizui, T., Takahashi, H., Sekino, Y., Shirao, T., 2005. Overexpression of drebrin A in immature neurons induces the accumulation of F-actin and PSD-95 into dendritic filopodia, and the formation of large abnormal protrusions. Mol. Cell. Neurosci. 30, 630–638.
Mizui, T., Sekino, Y., Yamazaki, H., Ishizuka, Y., Takahashi, H., Kojima, N., Kojima, M., Shirao, T., 2014. Myosin II ATPase activity mediates the long-term potentiation-induced exodus of stable F-actin bound by drebrin A from dendritic spines. PLoS One 9, e85367.
Nakagawa, T., Engler, J.A., Sheng, M., 2004. The dynamic turnover and functional roles of alpha-actinin in dendritic spines. Neuropharmacology 47, 734–745.
Noam, Y., Phan, L., McClelland, S., Manders, E.M., Ehrengruber, M.U., Wadman, W.J., Baram, T.Z., Chen, Y., 2012. Distinct regional and subcellular localization of the actin-binding protein filamin A in the mature rat brain. J. Comp. Neurol. 520, 3013–3034.
Shirao, T., 1995. The roles of microfilament-associated proteins, drebrins, in brain morphogenesis: a review. J. Biochem. 117, 231–236.
Shirao, T., Obata, K., 1986. Immunochemical homology of 3 developmentally regulated brain proteins and their developmental change in neuronal distribution. Dev. Brain Res. 29, 233–244.
Shirao, T., Kojima, N., Terada, S., Obata, K., 1990. Expression of three drebrin isoforms in the developing nervous system. Neurosci. Res. Suppl. 13, S106–S111.
Shirao, T., Hanamura, K., Koganezawa, N., Ishizuka, Y., Yamazaki, H., Sekino, Y., 2017. The role of drebrin in neurons. J. Neurochem. 141, 819–834.
Takabayashi, T., Xie, M.J., Takeuchi, S., Kawasaki, M., Yagi, H., Okamoto, M., Tariqur, R. M., Malik, F., Kuroda, K., Kubota, C., Fujieda, S., Nagano, T., Sato, M., 2010. LL5beta directs the translocation of filamin A and SHIP2 to sites of phosphatidylinositol 3,4,5-triphosphate (PtdIns(3,4,5)P_3) accumulation, and PtdIns(3,4,5)P_3 localization is mutually modified by co-recruited SHIP2. J. Biol. Chem. 285, 16155–16165.
Takahashi, H., Sekino, Y., Tanaka, S., Mizui, T., Kishi, S., Shirao, T., 2003. Drebrin-dependent actin clustering in dendritic filopodia governs synaptic targeting of postsynaptic density-95 and dendritic spine morphogenesis. J. Neurosci. 23, 6586–6595.
Tyler, W.J., Pozzo-Miller, L., 2003. Miniature synaptic transmission and BDNF modulate dendritic spine growth and form in rat CA1 neurones. J. Physiol. 553, 497–509.
Van Bommel, B., Konietzny, A., Kobler, O., Bär, J., Mikhaylova, M., 2019. F-actin patches associated with glutamatergic synapses control positioning of dendritic lysosomes. EMBO J. 38, e101183.
Xie, M.J., Ishikawa, Y., Yagi, H., Iguchi, T., Oka, Y., Kuroda, K., Iwata, K., Kiyonari, H., Matsuda, S., Matsuzaki, H., Yuzaki, M., Fukazawa, Y., Sato, M., 2019. PIP_3-Phldb2 is crucial for LTP regulating synaptic NMDA and AMPA receptor density and PSD95 turnover. Sci. Rep. 9, 4305.
Xie, M.J., Yagi, H., Kuroda, K., Wang, C.C., Komada, M., Zhao, H., Sakakibara, A., Miyata, T., Nagata, K., Oka, Y., Iguchi, T., Sato, M., 2013. WAVE2-Abi2 complex controls growth cone activity and regulates the multipolar-bipolar transition as well as the initiation of glia-guided migration. Cereb. Cortex 23, 1410–1423.
Yagi, H., Nagano, T., Xie, M.J., Ikeda, H., Kuroda, K., Komada, M., Iguchi, T., Tariqur, R. M., Morikubo, S., Noguchi, K., Murase, K., Okabe, M., Sato, M., 2014. Filamin A-interacting protein (FILIP) is a region-specific modulator of myosin 2b and controls spine morphology and NMDA receptor accumulation. Sci. Rep. 4, 6353.